Electronic Journal of Structural Engineering

Original Article

Cite this: DOI:10.56748/ejse.26974

Received Date: 08 February 2026
Accepted Date: 06 June 2026

1443-9255
https://ejsei.com/ejse

Comparative Numerical Analysis Study of the Lateral Performance of Steel Shear Walls with Dual-Layer Infill Plates

Qiaoqiao ZHANG [a b], Xiaosheng LIU [c*]

[a] School of Civil Engineering, Science and Technology College of Hubei University of Arts and Science, Xiangyang City, Hebei Province, 441025, China
[b] College of Civil Engineering & Architecture, China Three Gorges University, Yichang City, Hebei Province, 443002, China
[c] Department of Teaching and Scientific Research, Science and Technology College of Hubei University of Arts and Science, Xiangyang City, Hebei Province, 441025, China
* Corresponding author: LXSlgxy986@yeah.net

Abstract

Traditional steel shear walls (SSWs) with flat infill plates have been widely used in regions of high seismic hazard due to their high strength and energy dissipation capacity. However, premature buckling of flat plates reduces their structural performance, motivating the development of trapezoidal corrugated steel shear walls (CSSWs). To further address the limitations of single corrugated walls, double corrugated steel shear walls (DCSSWs) were introduced, followed by hybrid flat–corrugated steel shear walls (FCSSWs), which combine a flat plate with a trapezoidal corrugated plate. This study numerically investigates the lateral behavior of three SSW systems: single CSSWs, DCSSWs, and hybrid FCSSWs. Finite element models are developed using ABAQUS and analyzed under lateral loading. The effects of geometric parameters are examined by considering aspect ratios (L/h) ranging from 0.67 to 2 and corrugation angles of 30°, 45°, and 60°. The results indicate that dual-layer systems (DCSSW and FCSSW) significantly improve structural stability compared with single-layer CSSWs. Among the examined systems, the FCSSW exhibits the most stable nonlinear response, showing no strength degradation up to a 2% story drift. In contrast, the CSSW and the DCSSW with a 30° corrugation angle experience noticeable strength degradation. In terms of peak strength, the FCSSW consistently outperforms the CSSW, with the maximum increase (approximately 15.1%) observed at lower aspect ratios. The DCSSW achieves the highest ultimate strength, exceeding that of the FCSSW by 1.6–4.3% and the CSSW by 3.4–12.3%. Initial lateral stiffness is comparable among all systems, with only minor differences observed.

Keywords

Dual-layer steel shear wall, Flat-corrugated plates, Pushover, Resistance, Stiffness

1. Introduction

In contemporary times, the increasing population and expansion of urbanization have rendered the construction of high-rise structures capable of resisting lateral forces, particularly in seismically active regions, a principal challenge within civil engineering. Among the various structural systems, lateral load-resisting systems play a pivotal role in ensuring structural safety, stability, and optimal performance. Among these systems, steel shear walls (SSWs) have attracted considerable attention in both research and practical applications due to their significant advantages, including excellent ductile behavior, high energy dissipation capacity, superior strength-to-weight ratio, and rapid construction speed (Abdul Ghafar et al., 2022; He et al., 2025; Hosseinzadeh & Seddighi, 2024).

A conventional SSW system comprises a thin steel plate (serving as the primary shear-resisting element), horizontal boundary elements (beams), and vertical boundary elements (columns). The seismic behavior of this system is predominantly influenced by the shear buckling phenomenon of the infill plate (Driver, 1997; Habashi & Alinia, 2010). In unstiffened configurations, the plate, upon buckling, develops a diagonal tension field along its corners, which constitutes the primary source of the system's resistance and ductility. Although this post-buckling behavior is desirable, premature buckling can lead to a reduction in initial stiffness and pose serviceability concerns (Astaneh-Asl et al., 2019). To mitigate this challenge, various strategies have been proposed, including the use of stiffened plates with additional components (Alavi & Nateghi, 2013; Liu et al., 2024; Zhao et al., 2025) or the implementation of composite walls (Astaneh-Asl, 2002; Cheng et al., 2024; Pan et al., 2024). In this context, an innovative and effective solution involves the use of corrugated steel plates in lieu of flat plates (Dou et al., 2021, 2025). In this system, the steel plate is fabricated with a corrugated profile, typically sinusoidal or trapezoidal. This specific geometry significantly enhances the out-of-plane shear resistance of the plate, thereby effectively suppressing shear buckling at lower stress levels. The Corrugated Steel Shear Wall (CSSW) benefits from the key advantage of providing substantially higher initial stiffness (Emami et al., 2013; Qiu et al., 2018) and delaying the formation of the tension field without the need for intermediate stiffeners, which themselves increase construction complexity and cost. The conducted studies on the laboratory behavior of corrugated steel shear walls indicate that this system functions as a lateral load-resisting system with prominent mechanical properties, including high strength and stiffness, as well as high energy absorption capacity (E.-F. Deng et al., 2020; Feng et al., 2025; Li & Liu, 2025; Wen et al., 2025; Xie et al., 2024; Yu et al., 2022; X. Zhang et al., 2023). A corrugated steel plate is limited to a thickness of 8 mm (Wen et al., 2024) and, fundamentally, may not be suitable for use in tall structures subject to high shear forces. Furthermore, a single corrugated steel shear wall typically experiences a degradation in load-bearing capacity following out-of-plane buckling, resulting in a reduction in energy dissipation capability and ductility (Dou et al., 2018; Qiu et al., 2022). To overcome this issue, a double corrugated steel shear wall (DCSSW) system has been proposed (Tong et al., 2018; Tong, Guo, & Pan, 2020; Tong, Guo, Zuo, et al., 2020). This system consists of two identical trapezoidal corrugated steel plates connected using high-strength bolts. Deng et al. (R. Deng et al., 2022) conducted an experimental investigation on vertical DCSSWs and single CSSWs and concluded that the double-corrugated plate has a better shear stiffness and stable energy dissipation than the single-corrugated plate. Ghodratian-Kashan and Maleki (Ghodratian-Kashan & Maleki, 2022) conducted cyclic analysis on vertical DCSSWs and observed that DCSSWs had a spindle-shaped hysteresis curve with good cyclic performance. Corrugated plates can be installed vertically and horizontally inside the frame boundary element in corrugated walls. Recent research has proven that the seismic performance of the shear wall is optimal when the corrugation is placed vertically (R. Deng et al., 2023; Ghodratian-Kashan & Maleki, 2021; Zheng et al., 2022).

Recent developments have introduced innovative combined steel plate shear wall systems that integrate flat and corrugated steel plates to address the limitations of traditional configurations. These systems, known as flat-corrugated steel shear walls (FCSSWs), couple the plates to ensure combined action, resulting in several structural typologies: a four-layer assembly with a double-corrugated core between flat plates (Abbaszadeh et al., 2023; Broujerdian et al., 2021; Nayel et al., 2022; S. Zhang, 2025); a three-layer sandwich panel with a trapezoidal corrugated core (Dou et al., 2023); a two-layer wall combining flat and corrugated plates (Guan & Zhang, 2025; Lv, 2024, 2025). Lv introduced a two-layer steel shear wall consisting of one flat plate and one trapezoidal vertical corrugated plate with an aspect ratio of b/h = 1.56 (Fig. 1). They conducted cyclic loading tests on the numerical models using ABAQUS software. They found that the proposed systems enhanced the lateral behavior of the steel

shear wall system compared to traditional flat and single-corrugated steel shear walls. Guan (Guan & Zhang, 2025) investigated the cyclic performance of vertically- and horizontally placed two-layer steel shear walls with full, beam, and column-connected configurations with aspect ratio b/h=1. His exploration revealed that flat-corrugated configuration yields enhanced lateral performance compared to conventional flat and single-corrugated steel shear walls. Lv (Lv, 2025) found that the lateral resistance and energy dissipation of two-layer flat-corrugated steel shear walls with square openings are more than that of conventional steel shear walls.

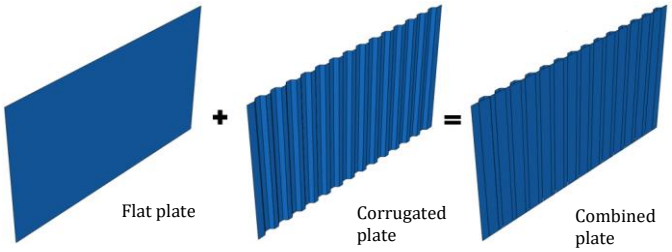

Fig. 1 The two-layer flat-corrugated plate (Lv, 2024).

Despite the demonstrated advantages of dual-layer steel shear walls, existing research has largely focused on either double-corrugated (DCSSW) or flat-corrugated (FCSSW) systems in isolation, often under limited geometric conditions. A critical gap remains in the direct comparative assessment of their lateral performance under consistent parameters, particularly regarding the coupled effects of varying aspect ratios and corrugation angles. Therefore, this study necessitates a systematic numerical investigation to compare the nonlinear behavior, strength degradation, and stiffness characteristics of CSSW, DCSSW, and FCSSW systems. The findings will provide essential guidance for selecting optimal dual-layer configurations for seismic-resistant design.

2. Method

2.1 Details of the Models

This study was conducted with the design of a single-bay and single-story CPSSW system according to the guidelines from the references (Farzampour et al., 2018; Yi et al., 2008). An infill plate with 8 mm thickness was selected. A W14×176 section and a W14×257 section was utilized for the frame beams and columns, respectively. Connections from beam to column are moment-resisting (rigid type). In this work, five aspect ratios (L/h) were considered, namely 0.67, 1, 1.33, 1.67, and 2 (see Fig. 2). The height for the infill plates (H) remains constant at 3000 mm in every model. Widths (L) of the infill plates with ratio L/h = 0.67, 1, 1.33, 1.67, and also 2 are given by: respectively, 2000; 3000; 4000; 5000; 6000 mm. This study gives an opportunity to evaluate the impact of the trapezoidal corrugation geometry parameters. The geometric specification for plates that are being investigated is demonstrated in Fig. 3. A value of 100 mm is decided for the width in both horizontal and diagonal flanges. For the corrugation angle, three different ones are analyzed, which are 30, 45, and 60 degrees.

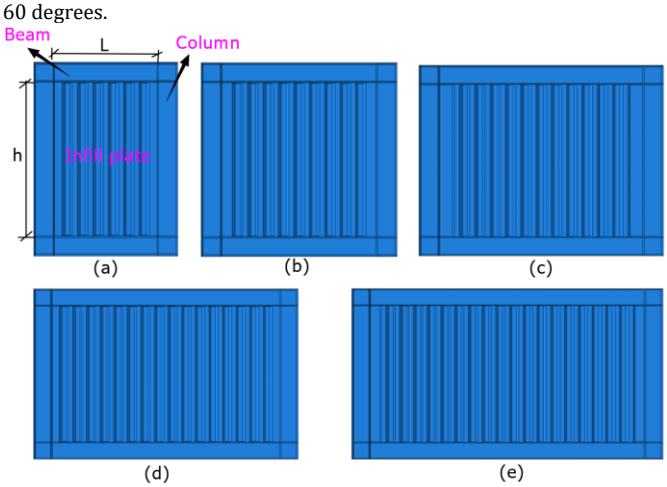

Fig. 2 The schematic shape of CSSWs with varing width-to-heigth L/h ratios, (a) L/h=0.67, (b) L/h=1, (c) L/h=1.33, (d) L/h=1.67, (e) L/h=2

In this paper, alongside the conventional vertical CSSW, a vertical DCSSW was considered as a control model. In this system, two vertically corrugated plates are utilized. The total thickness of both plates matches the 8 mm thickness found in the reference specimen, which gives a 4 mm thickness for each corrugated plate present in this dual-plate assembly. Additionally, a one FCSSW configuration that includes a flat plate combined with a trapezoidal corrugated plate is examined. The total thickness for plates in this setup remains at 8 mm. Each plate itself is 4 mm thick, so they measure this. Worth mentioning, characteristics for boundary frame members, such as beams together with columns, are being kept unchanged throughout all three systems under investigation. Some of these are single corrugated walls, double corrugated walls are included, and one is a type called flat corrugated walls.

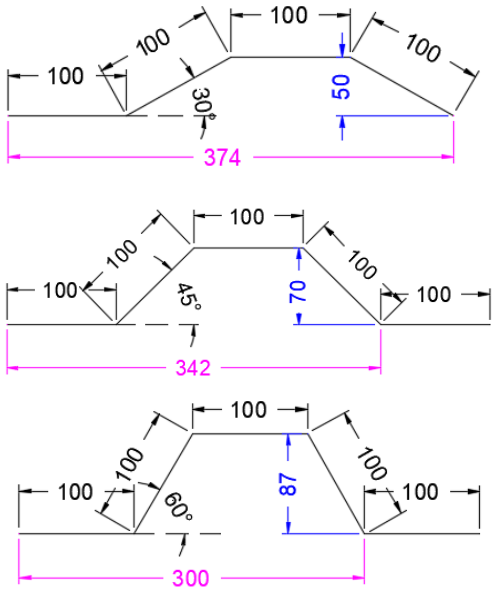

Fig. 3 The geometric properties of the trapezoidal corrugated plates

2.2 Finite Element Model

This part explains the establishment process for the computer model that uses the ABAQUS/Explicit software. The steel components were made with S4R shell elements with a mesh size of 25 mm according to mesh sensitivity analysis results, which contain four nodes, and use a reduced integration (Dou et al., 2023; Wu & Tong, 2025). The infill plates are connected to frame members by employing tie constraints (Dou et al., 2023; Feng et al., 2024). Connecting bolts, which connect the double-corrugated plates together with flat and corrugated plates, were not simulated directly in the ABAQUS software. Instead, the mentioned infill plates were coupled in the bolt locations in the FCSSW system. This is an established approach utilized in authoritative international references (R. Deng et al., 2022, 2023; Dou et al., 2023; Tong et al., 2018, 2023; Tong, Guo, & Pan, 2020; Tong, Guo, Zuo et al., 2020; Wen et al., 2024). To reflect the real-world construction imperfections, small initial deformations (h/750, where h is the plate height) give an opportunity to represent reality (Tong et al., 2023). The model relied on Q235 steel with a yield strength of 235 MPa. The stiffness value (E) selected is 206 GPa, and around 350 MPa for ultimate tensile strength. Steel acted in a bilinear manner and was considered for kinematic hardening. The Poisson ratio (ν) given to it is 0.3. Hardening modulus was set to be $E/100$, like in (Dou et al., 2023).

In Fig. 4, it can be seen that columns were fixed at the bottom part, while the top ends of the two side columns could not move in the sideways direction. At the upper beam, the horizontal load increased gradually until the structure reached two percent drift. The dynamic/implicit method was used to analyze the behavior of the studied models under lateral loads.

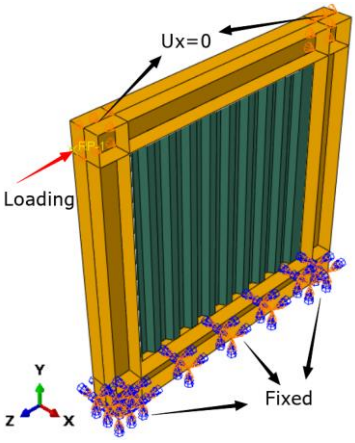

Fig. 4 Numerical model boundary constraints and lateral load arrangement

3. Validation of Numerical Models

3.1 Single-corrugated SSW

A vertical CSSW examined in the study by Emami et al. (Emami et al., 2013) was adopted for validation purposes in the present research. This specimen was subjected to cyclic loading using Abaqus software. Fig. 5 illustrates a comparison between the hysteresis curve derived from the experimental test and that obtained from the numerical analysis conducted in Abaqus. The comparison demonstrates strong alignment between the experimental results and the finite element model. Table 1 presents both the test and finite element (FE) outcomes. The discrepancies between the test and FE predictions for initial stiffness, peak resistance, and dissipated energy are 5.1%, 5.2%, and 3.2%, respectively. Furthermore, Fig. 6 compares the deformation patterns from the empirical and numerical models. Consistent with the experimental observations, plastic hinges formed at the column bases, a behavior accurately captured by the finite element model. Overall, the findings suggest that Abaqus software holds considerable promise for predicting the performance of CSSWs.

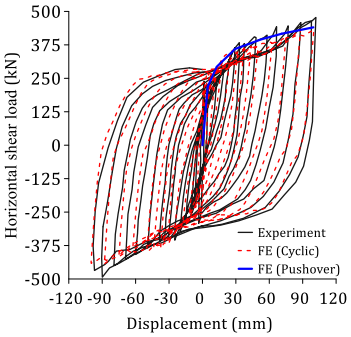

Fig. 5 Validation of CSSW versus test outcomes.

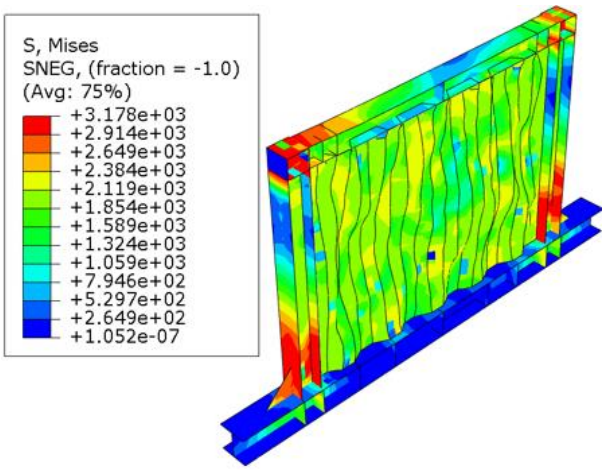

Fig. 6 Comparison of the failure mode of the test, and Von Mises stress of the FE modeling.

Table 1. The comparison of the test and FE results.

Model	Case	Test	FE	Error (%)
(Emami et al., 2013)	Initial stiffness (kN/mm)	105	110.3	5.1
	Peak resistance (kN)	490	465	5.2
	Dissipated energy (kJ)	550	567.3	3.2
(Ghodratian-Kashan & Maleki, 2022)	Initial stiffness (kN/mm)	105.3	101.3	3.7
	Peak resistance (kN)	365.0	383	4.9
	Dissipated energy (kJ)	296.0	315.3	6.5

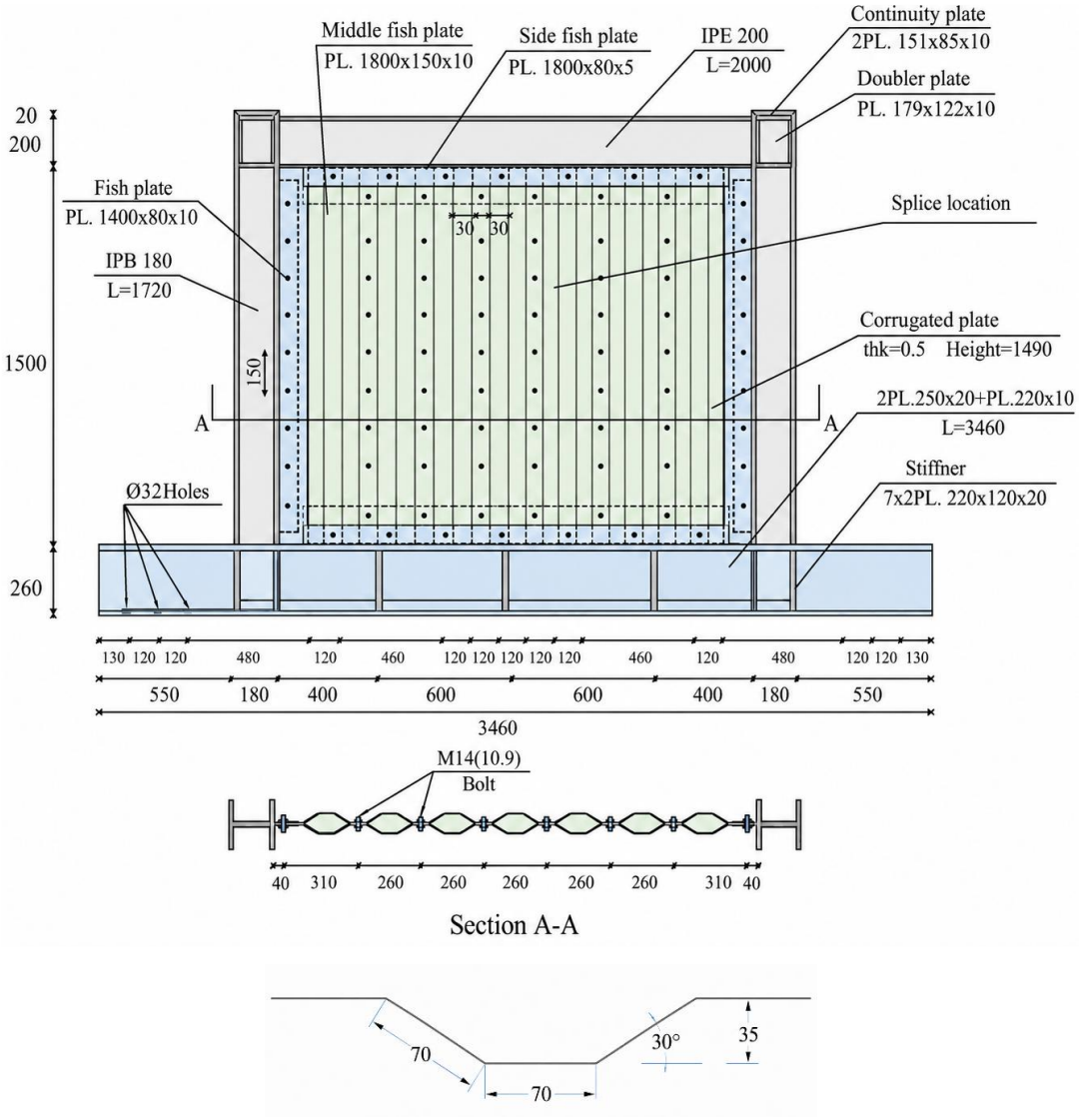

Fig. 7 The geometric features of the vertical DCSSWs test.

3.2 Double-corrugated SSW

In this section, a double-corrugated SSW tested by Ghodratian-Kashan and Maleki (Ghodratian-Kashan & Maleki, 2022) was simulated in ABAQUS software. The specimen configuration is illustrated in Fig. 7. This experimental unit contained a single-bay one-story framework. It is characterized by having a width measurement of 2.0 m as well as a vertical height equal to 1.72 m. The boundary frame consisted of an IPE200 top beam and IPB180 side columns, all of which were fixed to a plate girder base beam anchored to the strong floor. Moment-resisting welded and unreinforced flange connections are being used in junctures between the beam and column. The infill shear wall was constructed by employing two identical trapezoidal corrugated plates of thickness 0.5 mm, with overall measurements of 1490 × 1990 mm. The corrugation profile has been defined by an angle of 30 degrees. The sub-plate width can be flat or inclined, measuring 70 mm. Infill plates were systematically interconnected and fixed to the boundary frame with fishplates and some high-strength M14 (10.9) bolts distributed at regular intervals. The characteristics of the material for these components are given in Table 2.

Table 2. Material features of the test elements (Ghodratian-Kashan & Maleki, 2022).

Element	Ultimate stress F_u (MPa)	Yield stress F_y (MPa)	Percent elongation (%)
Column	455.7	277.8	28.6
Beam	461.9	330.1	30.4
plate	383.5	328.2	39.6

Fig. 8 shows how highly the computer model corresponds to the real experiment when monotonic loading is applied. The hysteresis curves from both the test and FE analysis are in close agreement. As per Table 1, the difference between initial stiffness, peak resistance, and dissipated energy of the test and FE models is 3.7%, 4.9%, and 6.5%, respectively. The deformed shape that ABAQUS predicts also matches what was detected in the actual test specimen after the loading process. Such comparisons give evidence that ABAQUS can successfully predict how the system of DCSSW behaves under lateral loads.

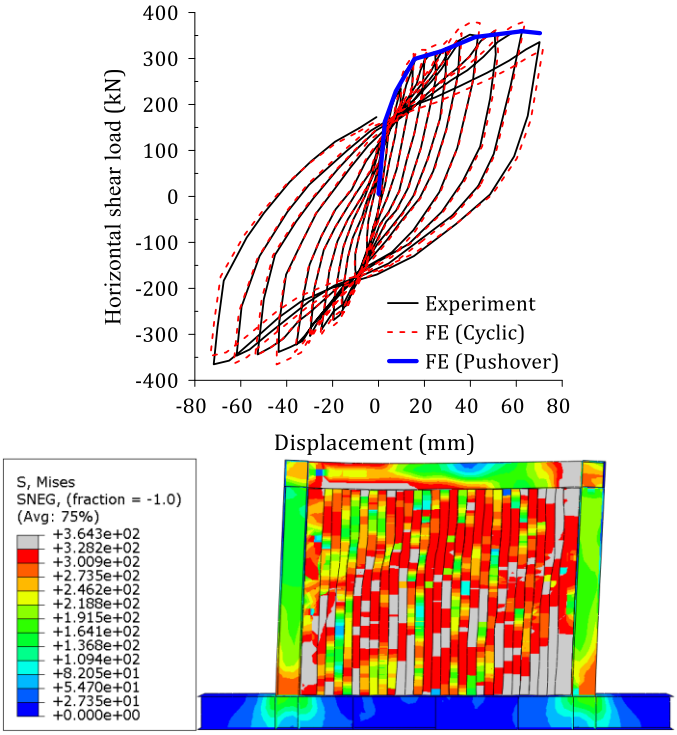

Fig. 8 Comparison of the experimental and FE results.

It should be noted that, since the mesh size has a significant effect on the results, a mesh sensitivity analysis was performed on the two specimens considered for calibration. The results of this analysis are presented in Fig. 9. As the maximum strength did not change for mesh sizes smaller than 25 mm, a mesh size of 25 mm was adopted in this study for modeling the specimens under investigation.

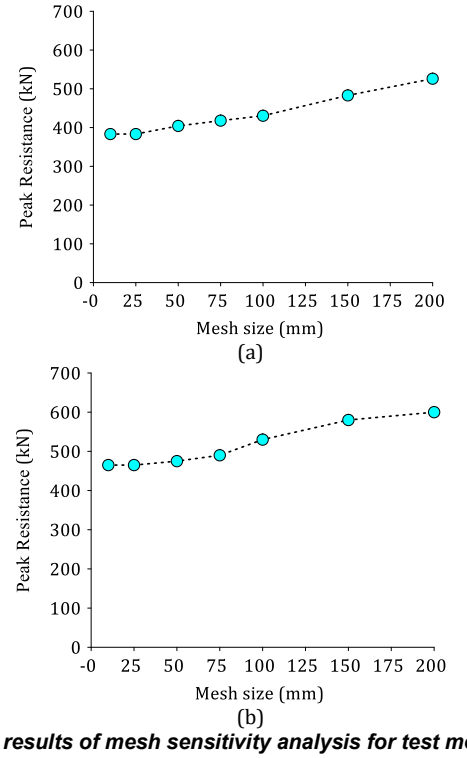

Fig. 9 The results of mesh sensitivity analysis for test models of (a) Emami et al. (Emami et al., 2013) and (b) Ghodratian-Kashan and Maleki(Ghodratian-Kashan & Maleki, 2022).

4. Results and Discussion

4.1 Pushover Curves

The pushover curves and numerical samples for various aspect ratios are presented in Fig. 10. It should be noted that the vertical axis of the pushover curves is presented as $\frac{V}{V_y}$, where V is the shear load applied to the models, and V_y is the full-section shear yield strength (Dou et al., 2023). V_y is expressed as $V_y = tLf_y/\sqrt{3}$, where t is the plate thickness, L is the bay width, and f_y is the yield stress of the infill plates.

As observed, in single-corrugated walls, a degradation in the load-displacement curve occurs, particularly when the corrugation angle is small (here, 30 degrees). This degradation manifests with greater intensity and steepness at higher aspect ratios. In contrast, double-corrugated walls show strength degradation exclusive to specimens having a corrugation angle of 30 degrees, and this effect gets more noticeable when the aspect ratio is increased. A major aspect for the comparison among load-displacement curves of both systems is that in double-corrugated walls, there is a gradual occurrence of strength degradation rather than it occurring faster, as seen in single-corrugated walls. From this, it tells that in the nonlinear part, double-corrugated walls are steadier and more ductile when compared to using single-corrugated walls and also have better dissipation for energy. Meanwhile, flat-corrugated walls exhibit no strength degradation, even at the final loading stage (corresponding to a 2% drift). This demonstrates that a double-layered flat-corrugated wall, composed of one flat and one trapezoidal corrugated plate, exhibits more stable nonlinear behavior than both single- and double-corrugated trapezoidal walls. Such high-quality performance kind of helps explain strong suitability for those high-seismic areas since more energy can be dissipated in those places.

4.2 Peak Resistance

Fig. 11 presents a comparative analysis of the peak shear resistance derived from the numerical models. The term peak resistance refers to the ultimate bearing capacity exhibited by the structure during loading, from zero drift up to the allowable drift of 2%. For a more effective comparison, a pairwise analysis of the tests is presented in Fig. 12. Fig. 12a shows a comparison of the strength between FCSSW and CSSW. Fig. 12b presents a comparison of the strength between FCSSWs and DCSSWs. Fig. 12c reveals that the DCSSWs are compared with single-corrugated ones for ultimate strength.

Fig. 12a shows that flat-corrugated walls consistently show better performance than single-corrugated walls for strength, with a maximum difference of up to 15.1%. The recorded average strength benefits are 5.2%, 6.8%, 3.8%, 1.3%, and also 0.1% for L/H ratios equal to 0.67, 1, 1.33, 1.67, and 2, respectively. The results indicate that higher aspect ratios give an opportunity to access reduced differences in strength, which become

almost insignificant at the L/H values of both 1.67 and at the level of 2. This suggests that at a level of 2, strength gains are minimal.

With reference to Fig. 12b, which represents the strength ratio of the FCSSW to the DCSSW, it is evident that the double-corrugated walls exhibit higher ultimate strength than the flat-corrugated walls. However, the distinction in the ultimate strength among these two systems is 1.6%, 4.3%, 3.6%, 2.3%, and also 3.2% when the aspect ratios are 0.67, 1, 1.33, 1.67, and also 2, respectively. Thus, with respect to strength, a significant difference does not appear to exist between a DCSSW system and the FCSSW system.

In relation to Fig. 12c, which shows the strength proportion of double-corrugated to single-CSSW, one can see that the DCSSWs have more strength compared to ordinary single-corrugated wall structures. The difference in ultimate strength between these two systems is 7.1%, 12.3%, 7.9%, 3.8%, and 3.4% for the respective aspect ratios. It is evident that the strength differential between the two systems rises as the aspect ratio rises from 0.67 to 1 and subsequently decreases. Beyond that, Fig. 12c shows that an increase in the corrugation angle gives an opportunity to access a reduction in the strength difference between the two systems.

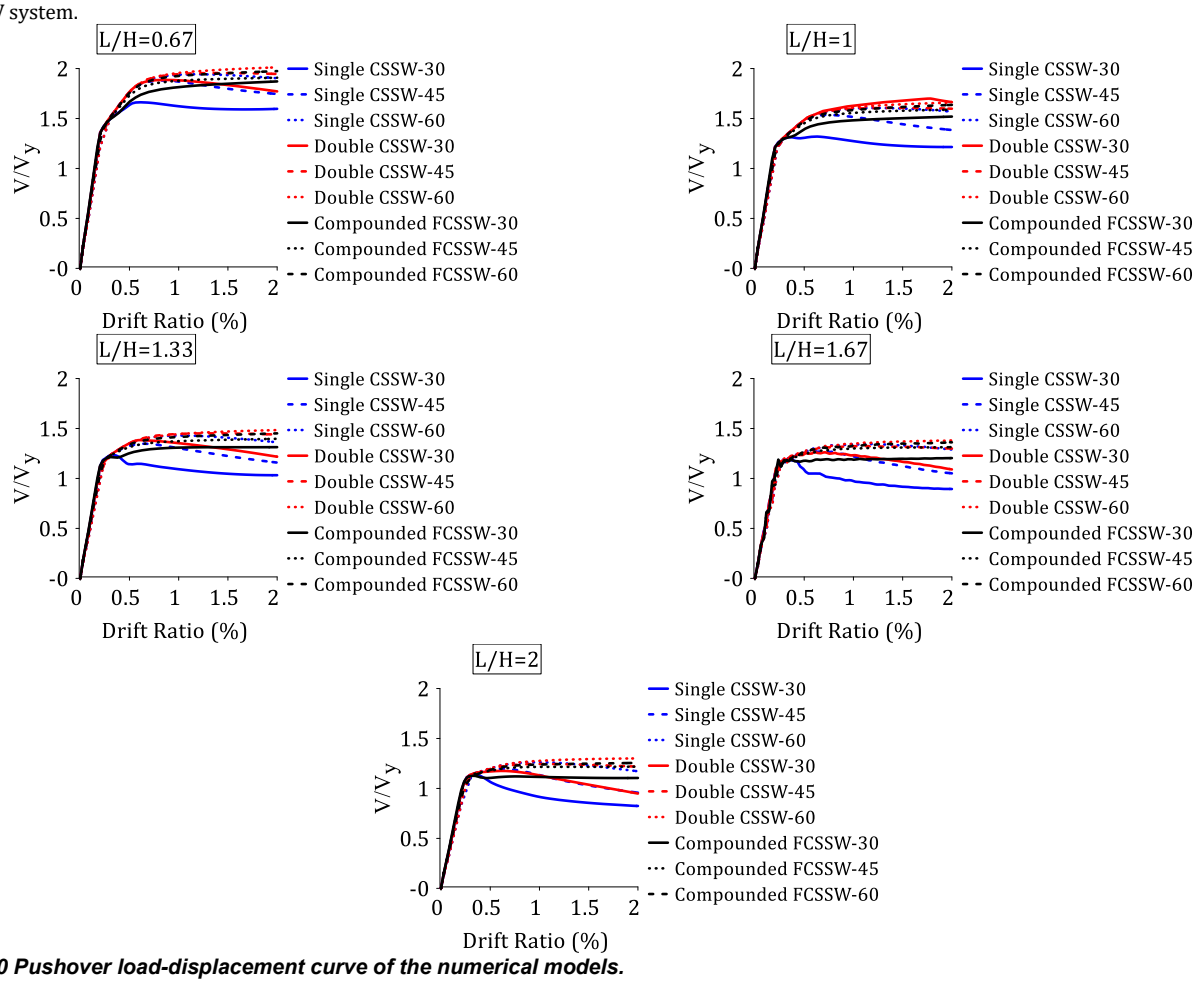

Fig. 10 Pushover load-displacement curve of the numerical models.

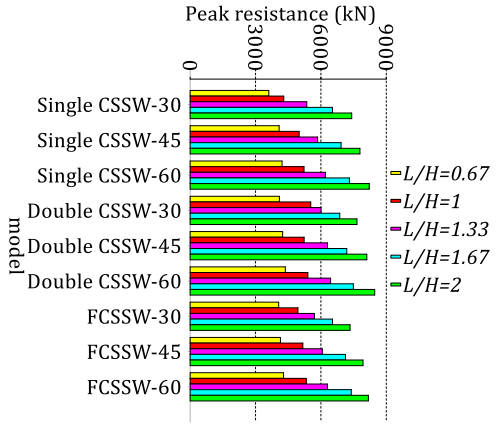

Fig. 11 Comparative analysis of the ultimate resistance exhibited by the numerical models

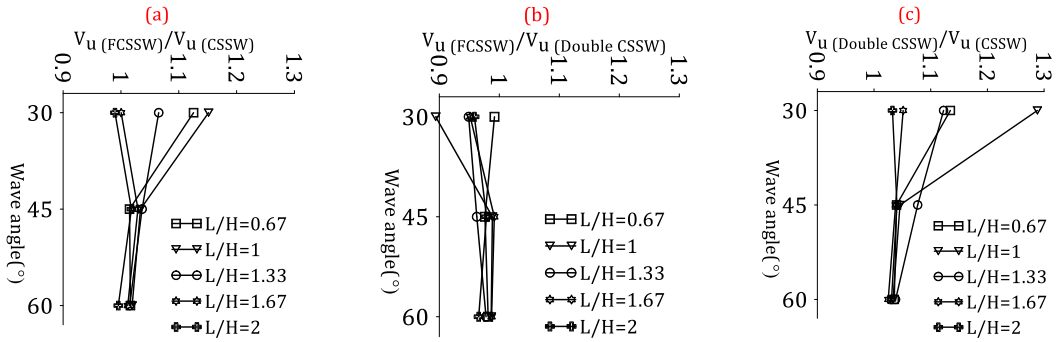

Fig. 12 The Ratio of the ultimate resistance

4.3 Lateral Stiffness

Fig. 13 presents degradation curves for the lateral stiffness regarding the specimens studied at various width-to-height ratios. As observed, the lateral stiffness continuously decreases with increasing drift. This part investigates initial stiffness (IS), which is the stiffness measured at the elastic stage of the load-displacement curve. Fig. 14 shows a comparison of the initial stiffness for all specimens, showing that only minor differences are present. Fig. 15 gives pairwise ratios of stiffness: flat-corrugated to single-corrugated (Fig. 15a), flat-corrugated to double-corrugated (Fig. 15b), and double-corrugated to single-corrugated (Fig. 15c).

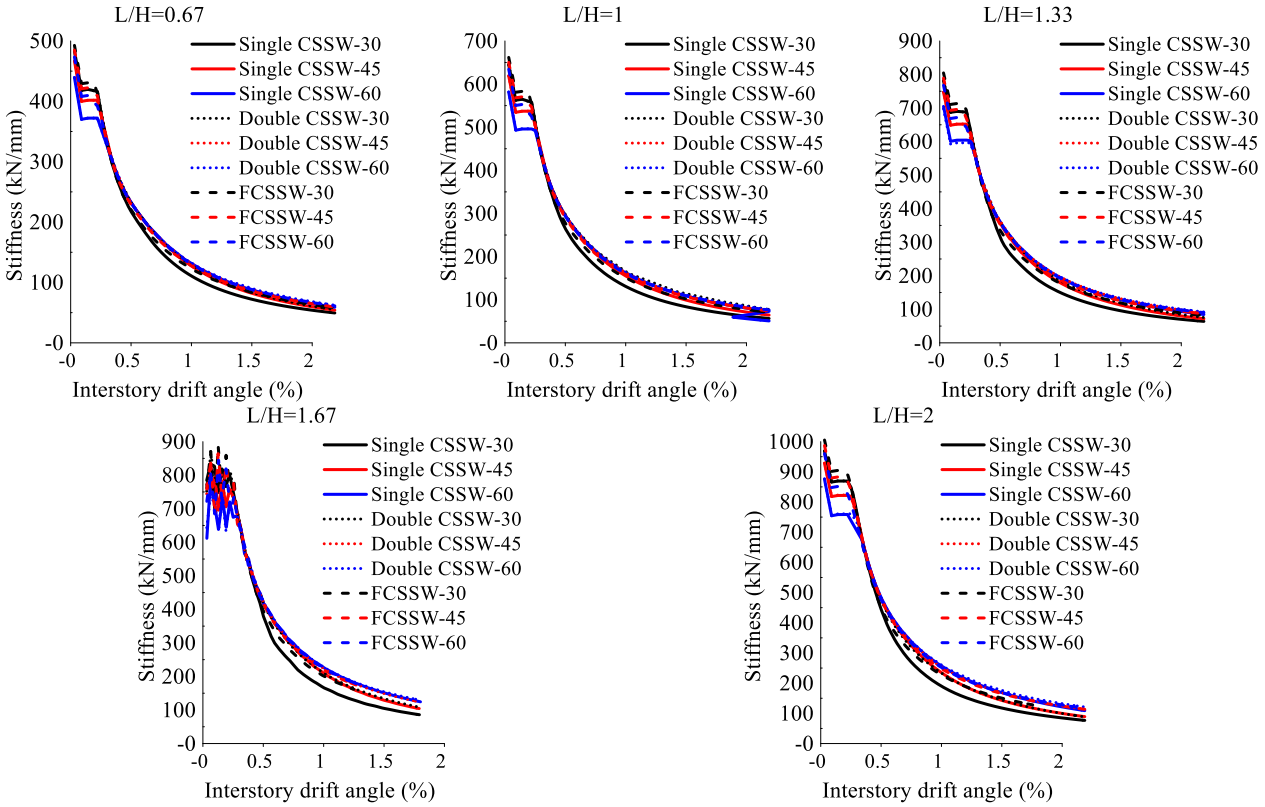

Fig. 13 The stiffness deterioration curve of the numerical models

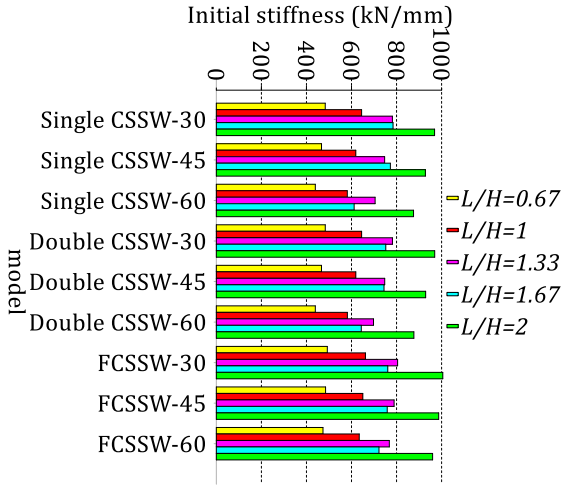

Fig. 14 The comparison of the initial stiffness of the numerical models

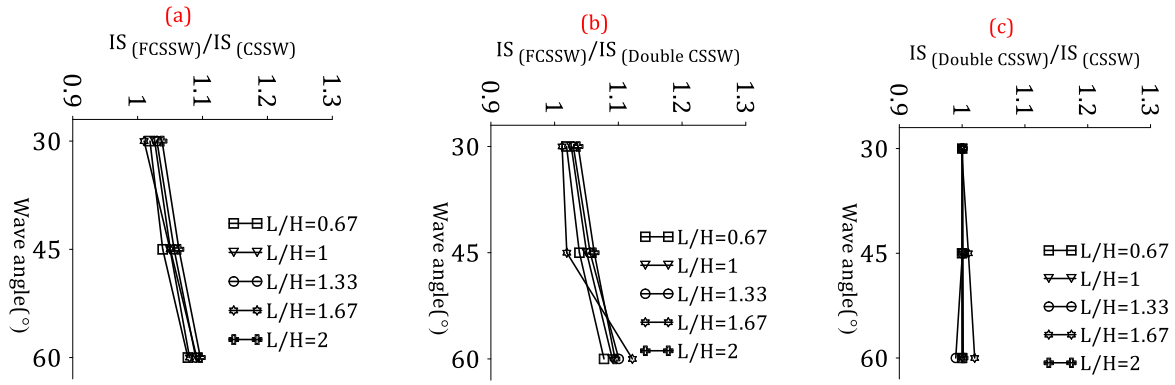

Fig. 15 The Ratio of the initial stiffness.

4.4 Residual Resistance

In this section, the residual strength of the studied specimens is examined, as depicted in Fig. 16. Residual strength refers to the strength corresponding to the ultimate drift of 2%. As observed, the residual strength in double-corrugated and flat-corrugated walls is greater than that in conventional single-corrugated walls. The residual strength in double-corrugated walls is between 5.6% and 49.8% higher than that in single-corrugated walls. Furthermore, the residual strength in flat-corrugated walls is between 3.7% and 47.9% higher than that in single-corrugated walls. Meanwhile, the difference in residual strength between double-corrugated and flat-corrugated walls ranges from 8.6% to 16.4% (mean value: 10.1%). These differences clearly indicate the higher capacity of double-corrugated and flat-corrugated walls compared to conventional single-corrugated steel shear walls in providing superior energy dissipation capacity and ductility.

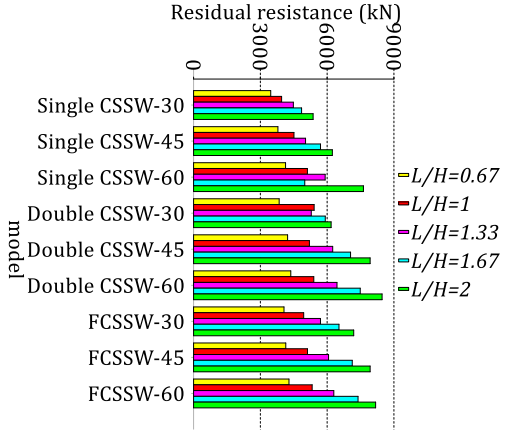

Fig. 16 Comparative analysis of the residual resistance exhibited by the numerical models.

4.5 Deformations

The current section shows deformation properties of the given numerical models. Specifically, it examines out-of-plane displacement allocation for cases that possess an aspect ratio of b/h = 1 and a corrugation angle equal to 30°. The deformation structures that belong to CSSW, DCSSW, and FCSSW types can be seen in Fig. 17a, 17b, and 17c separately. Results indicate there are considerably higher out-of-plane displacements for a single corrugated steel wall (CSSW) than for other systems. This finding gives an opportunity to infer that the usage of dual-layer steel plate configurations especially reduces out-of-plane deformation on infill plates as compared with a conventional single corrugated wall system.

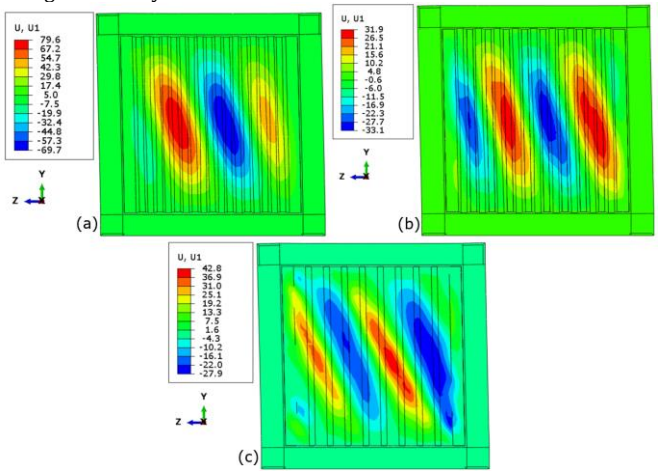

Fig. 17 The distributions of out-of-plane displacement, (a) CSSW, (b) DCSSW, (c) FCSSW.

5. Design Assumptions, Methodology, and Practical Optimization for the Proposed System

The numerical methodology employed in this study is predicated on several key design assumptions. First, the infill plates and boundary frames (W14×176 beams and W14×257 columns) are assumed to be perfectly connected using tie constraints. In contrast, the bolted connections between dual-layer plates (in DCSSW and FCSSW) are idealized by coupling degrees of freedom at bolt locations, an approach validated in prior studies (R. Deng et al., 2022, 2023; Dou et al., 2023; Tong et al., 2018, 2023; Tong, Guo, & Pan, 2020; Tong, Guo, Zuo, et al., 2020; Wen et al., 2024). Second, a bilinear kinematic hardening material model with a hardening modulus of E/100 is assumed for Q235 steel (yield strength 235 MPa, E=206 GPa), and geometric imperfections of h/750 are introduced to simulate realistic initial out-of-plane deformations. The methodology consists of developing validated ABAQUS/Explicit models using S4R shell elements with a 25 mm mesh (determined via mesh sensitivity analysis) and applying monotonic pushover loading up to a 2% story drift under fixed-bottom boundary conditions. For practical applications, optimal considerations indicate that the hybrid flat-corrugated steel shear wall (FCSSW) offers the most stable nonlinear response with no strength degradation up to 2% drift, making it ideal for high-seismic regions. While the double-corrugated (DCSSW) system achieves marginally higher ultimate strength (1.6–4.3% greater than FCSSW), the FCSSW is preferred for its superior energy dissipation and post-yield stability. Aspect ratios (L/h) above 1.67 yield diminishing strength gains for dual-layer systems, and a corrugation angle of 30° should be avoided in single or double corrugated walls due to noticeable strength degradation. Future research should focus on: (1) experimental validation of the FCSSW under cyclic loading to confirm its stable hysteretic response; (2) optimization of corrugation geometry (angle, wavelength, and depth) to maximize strength-to-weight ratios; (3) investigating the effect of openings (e.g., doors, windows) on the lateral performance of FCSSW systems; and (4) developing simplified design equations and seismic force modification factors for incorporation into building codes.

6. Conclusion

This comparative numerical study provides quantitative evidence of the superior lateral performance of dual-layer infill plate systems compared to single-CSSWs. The pushover analysis revealed that the FCSSW exhibited the most stable load-displacement behavior, showing no strength degradation up to the 2% drift limit, unlike the single- and double-corrugated walls, which experienced post-peak strength drops, particularly at lower corrugation angles (e.g., 30°) and higher aspect ratios. Quantitatively, the ultimate shear resistance of the FCSSW was consistently higher than that of the single-corrugated wall, with the percentage increase ranging from 0.1% to 6.8% across different aspect ratios (L/h = 0.67 to 2), averaging a 3.4% improvement. While the double-corrugated wall showed a marginally higher peak resistance than the FCSSW (by 1.6% to 4.3%), the difference was negligible, indicating that the FCSSW achieves a comparable strength level. More especially, resistance for a double-corrugated wall was from 3.4% to 12.3% greater than that of the single-corrugated wall, which highlights the benefit of adding a second plate. Regarding initial stiffness, the comparative ratios (FCSSW/single, FCSSW/double, and double/single) consistently hovered near 1.0 across all configurations, indicating that all three systems possess comparable initial elastic stiffness. Therefore, the key quantitative differentiator is the enhanced post-yield stability and energy dissipation capacity of the FCSSW, making it the most favorable configuration for high-seismic applications where stable, ductile performance is paramount.

Authorship Contribution Statement

Xiaosheng LIU: Conceptualization, Supervision, Project administration, Writing-Original draft preparation.
Qiaoqiao ZHANG: Validation, Software, Methodology.

Data Availability

Accessible upon formal inquiry.

Conflicts of Interest

The authors affirm the absence of any conflict of interest pertaining to the dissemination of this manuscript.

References

Abbaszadeh, A., Ghamari, A., & Broujerdian, V. (2023). Seismic behavior of an innovative four-layer steel shear wall. KSCE Journal of Civil Engineering, 27(11), 4770-4786.https://doi.org/10.1007/s12205-023-1419-8

Abdul Ghafar, W., Tao, Z., Tao, Y., He, Y., Wu, L., & Zhang, Z. (2022). Experimental and numerical study of an innovative infill web-strips steel plate shear wall with rigid beam-to-column connections. Buildings, 12(10), 1560.https://doi.org/10.3390/buildings12101560

Alavi, E., & Nateghi, F. (2013). Experimental study on diagonally stiffened steel plate shear walls with central perforation. Journal of

Constructional Steel Research, 89, 9-20. https://doi.org/10.1016/j.jcsr.2013.06.005

Astaneh-Asl, A. (2002). Seismic behavior and design of composite steel plate shear walls. Structural Steel Educational Council Moraga, CA, USA. https://doi.org/10.1016/S0143-974X(01)00101-8

Astaneh-Asl, A., Qian, X., & Shi, Y. (2019). Application of steel shear walls toward more resilient structures. In Resilient structures and infrastructure (pp. 3-46). Springer. https://doi.org/10.1007/978-981-13-7446-3_1

Broujerdian, V., Ghamari, A., & Abbaszadeh, A. (2021). Introducing an efficient compound section for steel shear wall using flat and corrugated plates. Structures, 33, 2855-2871. https://doi.org/10.1016/j.istruc.2021.06.027

Cheng, Y., He, H., Sun, H., & Li, J. (2024). Seismic experiment and performance analysis on embedded optimized steel plate-reinforced concrete composite shear wall under multi-dimensional loading. Journal of Building Engineering, 98, 111087. https://doi.org/10.1016/j.jobe.2024.111087

Deng, E.-F., Zong, L., Wang, H.-P., Shi, F.-W., & Ding, Y. (2020). High efficiency analysis model for corrugated steel plate shear walls in modular steel construction. Thin-Walled Structures, 156, 106963. https://doi.org/10.1016/j.tws.2020.106963

Deng, R., Yang, J.-D., Wang, Y.-H., Li, Q.-Q., & Tan, J.-K. (2022). Cyclic shear performance of built-up double-corrugated steel plate shear walls: Experiment and simulation. Thin-Walled Structures, 181, 110077. https://doi.org/10.1016/j.tws.2022.110077

Deng, R., Yang, J.-D., Wang, Y.-H., Li, Q.-Q., Yu, Z., Shen, Q.-W., & Yang, Y. (2023). Buckling and ultimate resistance of double-corrugated steel plates under in-plane shear load. Structures, 53, 1267-1282. https://doi.org/10.1016/j.istruc.2023.05.012

Dou, C., Cheng, X., Zhao, Y.-Y., & Yang, N. (2021). Shear resistance and design of infill panels in corrugated-plate shear walls. Journal of Structural Engineering, 147(11), 04021179. https://doi.org/10.1061/(ASCE)ST.1943-541X.0003162

Dou, C., Pi, Y.-L., & Gao, W. (2018). Shear resistance and post-buckling behavior of corrugated panels in steel plate shear walls. Thin-Walled Structures, 131, 816-826. https://doi.org/10.1016/j.tws.2018.07.039

Dou, C., Xie, C., Wang, Y., & Yang, N. (2023). Cyclic loading test and lateral resistant behavior of flat-corrugated steel plate shear walls. Journal of Building Engineering, 66, 105831. https://doi.org/10.1016/j.jobe.2023.105831

Dou, C., Zhang, J., Lan, T., Wang, D., & Zhang, G. (2025). Elastic shear buckling analysis of infill panels in trapezoidal corrugated plate shear walls. Thin-Walled Structures, 215, 113452. https://doi.org/10.1016/j.tws.2025.113452

Driver, R. G. (1997). Seismic behaviour of steel plate shear walls.

Emami, F., Mofid, M., & Vafai, A. (2013). Experimental study on cyclic behavior of trapezoidally corrugated steel shear walls. Engineering Structures, 48, 750-762. https://doi.org/10.1016/j.engstruct.2012.11.028

Farzampour, A., Mansouri, I., Lee, C.-H., Sim, H.-B., & Hu, J. W. (2018). Analysis and design recommendations for corrugated steel plate shear walls with a reduced beam section. Thin-Walled Structures, 132, 658-666. https://doi.org/10.1016/j.tws.2018.09.026

Feng, L., Yang, H., Sun, T., & Ou, J. (2024). Experimental and numerical studies on cyclic behavior of stiffened corrugated steel plate shear walls with different corrugation orientations. Earthquake Engineering & Structural Dynamics, 53(8), 2511-2531. https://doi.org/10.1002/eqe.4123

Feng, L., Yang, H., Wang, J. O. Q., & Sune, M. (2025). Shear resistance and design of horizontally placed stiffened corrugated steel plate shear walls. Steel and Composite Structures, 55(6), 473.

Ghodratian-Kashan, S. M., & Maleki, S. (2021). Numerical investigation of double corrugated steel plate shear walls. Journal of Civil Engineering and Construction, 10(1), 44-58. https://doi.org/10.32732/jcec.2021.10.1.44

Ghodratian-Kashan, S. M., & Maleki, S. (2022). Experimental investigation of double corrugated steel plate shear walls. Journal of Constructional Steel Research, 190, 107138. https://doi.org/10.1016/j.jcsr.2022.107138

Guan, Z., & Zhang, L. (2025). On the Hysteretic Behavior of Fully Connected and Beam-Connected Flat-Corrugated Steel Shear Walls with Different Corrugation Angles and Orientations. Electronic Journal of Structural Engineering, 25(2), 33-39. https://doi.org/10.56748/ejse.24815

Habashi, H. R., & Alinia, M. M. (2010). Characteristics of the wall-frame interaction in steel plate shear walls. Journal of Constructional Steel Research, 66(2), 150-158. https://doi.org/10.1016/j.jcsr.2009.09.004

He, J., Wang, L., Hu, J., He, Z., & Chen, S. (2025). Optimization of Slotted Steel Plate Shear Walls Based on Adaptive Genetic Algorithm. Applied Sciences, 15(11), 6088. https://doi.org/10.3390/app15116088

Hosseinzadeh, S. A. A., & Seddighi, M. (2024). Wall-frame interactive behavior in GFRP-reinforced steel plate shear walls with circular cutout openings. Structures, 61, 106061. https://doi.org/10.1016/j.istruc.2024.106061

Li, S.-D., & Liu, X.-G. (2025). Experimental investigation of innovative high-bearing and large-deformation steel plate shear wall utilizing trapezoidal corrugated panel. Thin-Walled Structures, 209, 112950. https://doi.org/10.1016/j.tws.2025.112950

Liu, B.-Z., Tong, G.-S., Tong, J.-Z., Xu, Z.-Y., & Hou, J. (2024). Shear stability and resistance design of novel vertically flexible stiffened steel plate shear walls. Structures, 59, 105694. https://doi.org/10.1016/j.istruc.2023.105694

Lv, P. (2024). Investigating the behavior of a steel shear wall consisting of a corrugated and flat plate with fully and semi connections to boundary elements. Multiscale and Multidisciplinary Modeling, Experiments and Design, 7(4), 3827-3839. https://doi.org/10.1007/s41939-024-00445-z

Lv, P. (2025). Cyclic Behavior of Two-Layer Flat-CSSWs with Square Opening. International Journal of Steel Structures, 25(3), 591-608. https://doi.org/10.1007/s13296-025-00958-4

Nayel, I. H., Ghamari, A., & Broujerdian, V. (2022). On the behavior of an innovative four-layer semi-supported steel plate shear wall. Case Studies in Construction Materials, 17, e01427. https://doi.org/10.1016/j.cscm.2022.e01427

Pan, Z., Si, D., Jiang, S., Huang, Z., & Meng, S. (2024). Numerical and experimental investigation on composite shear walls with different steel layouts. Journal of Constructional Steel Research, 219, 108760. https://doi.org/10.1016/j.jcsr.2024.108760

Qiu, J., Zhao, Q., Yu, C., & Li, Z. (2018). Experimental studies on cyclic behavior of corrugated steel plate shear walls. Journal of Structural Engineering, 144(11), 04018200. https://doi.org/10.1061/(ASCE)ST.1943-541X.0002165

Qiu, J., Zhao, Q., Yu, C., & Wang, Z. (2022). Lateral behavior of trapezoidally corrugated wall plates in steel plate shear walls, Part 2: Shear strength and post-peak behavior. Thin-Walled Structures, 174, 109103. https://doi.org/10.1016/j.tws.2022.109103

Tang, G., Yin, L., Guo, X., & Cui, J. (2015). Finite element analysis and experimental research on mechanical performance of bolt connections of corrugated steel plates. International Journal of Steel Structures, 15, 193-204. https://doi.org/10.1007/s13296-015-3014-4

Tong, J.-Z., Guo, Y.-L., & Pan, W.-H. (2020). Ultimate shear resistance and post-ultimate behavior of double-corrugated-plate shear walls. Journal of Constructional Steel Research, 165, 105895. https://doi.org/10.1016/j.jcsr.2019.105895

Tong, J.-Z., Guo, Y.-L., & Zuo, J.-Q. (2018). Elastic buckling and load-resistant behaviors of double-corrugated-plate shear walls under pure in-plane shear loads. Thin-Walled Structures, 130, 593-612. https://doi.org/10.1016/j.tws.2018.06.021

Tong, J.-Z., Guo, Y.-L., Zuo, J.-Q., & Gao, J.-K. (2020). Experimental and numerical study on shear resistant behavior of double-corrugated-plate shear walls. Thin-Walled Structures, 147, 106485. https://doi.org/10.1016/j.tws.2019.106485

Tong, J.-Z., Wu, R.-M., Xu, Z.-Y., & Guo, Y.-L. (2023). Subassemblage tests on seismic behavior of double-corrugated-plate shear walls. Engineering Structures, 276, 115341. https://doi.org/10.1016/j.engstruct.2022.115341

Wen, C.-B., Zhu, B.-L., Sun, H.-J., Guo, Y.-L., Zheng, W.-J., & Deng, L.-L. (2024). Global stability design of double corrugated steel plate shear walls under combined shear and compression loads. Thin-Walled Structures, 199, 111789. https://doi.org/10.1016/j.tws.2024.111789

Wen, C.-B., Zuo, J.-Q., Guo, Y.-L., He, X., Sun, H.-J., & Duan, J.-S. (2025). Experimental and numerical study on seismic behaviors of corrugated plate shear walls. Journal of Constructional Steel Research, 229, 109496. https://doi.org/10.1016/j.jcsr.2025.109496

Wu, R.-M., & Tong, J.-Z. (2025). Shear strength and post-ultimate behavior of multi-stiffened corrugated steel plate shear walls. Journal of Constructional Steel Research, 229, 109480. https://doi.org/10.1016/j.jcsr.2025.109480

Xie, Z., Shi, L., Peng, L., Zhang, S., Zhou, D., Zhang, X., & Yu, C. (2024). Behaviour of a cold-formed steel shear wall with centre-corrugated steel sheathing under cyclic loading. Engineering Structures, 318, 118650. https://doi.org/10.1016/j.engstruct.2024.118650

Yi, J., Gil, H., Youm, K., & Lee, H. (2008). Interactive shear buckling behavior of trapezoidally corrugated steel webs. Engineering Structures, 30(6), 1659-1666. https://doi.org/10.1016/j.engstruct.2007.11.009

Yu, Y., Lin, S., Zhao, F., Tian, P., & Jiang, L. (2022). A built-up type of horizontally corrugated steel plate shear wall with a special shape. Engineering Structures, 250, 113458. https://doi.org/10.1016/j.engstruct.2021.113458

Zhang, S. (2025). Improving the structural performance of steel shear wall systems with four-layer flat-corrugated steel plates in construction

engineering. International Journal of Mechanics and Materials in Design, 1-15. https://doi.org/10.1007/s10999-025-09807-y

Zhang, X., Chen, Y., Qiao, H., Kong, W., Zhang, C., Pan, J., & Zhang, W. (2023). Investigation on hysteretic performance of assembled H-shaped steel frame-corrugated steel plate shear wall with different corrugated orientation and wavelength. Journal of Building Engineering, 77, 107473. https://doi.org/10.1016/j.jobe.2023.107473

Zhao, C., Yu, J., & Zhong, W. (2025). Experimental study of oblique multi-rib stiffened steel plate shear wall with four-corner connection. Journal of Building Engineering, 108, 112891. https://doi.org/10.1016/j.jobe.2025.112891

Zheng, L., Wang, W., Ge, H., Guo, H., Gao, Y., & Han, Y. (2022). Seismic performance of steel corrugated plate structural walls with different corrugation inclinations. Journal of Constructional Steel Research, 192, 107248. https://doi.org/10.1016/j.jcsr.2022.107248

Disclaimer